Seeing in the dark: Vectashield quenches Alexa Fluor 647 fluorescence, but does not hinder dSTORM imaging

Aleksandra Arsić[1#], Nevena Stajković[1#], Rainer Spiegel[2], Ivana Nikić-Spiegel[1*]

[1]Werner Reichardt Centre for Integrative Neuroscience, University of Tübingen, Germany

[2]BG Hospital Tübingen, University of Tübingen, Germany

[#]equal contribution

[*]correspondence should be addressed to Ivana Nikić-Spiegel, ivana.nikic@cin.uni-tuebingen.de

Abstract

It was recently reported that Vectashield, a commercial mounting medium, can be used for direct stochastic optical reconstruction microscopy (dSTORM) of Alexa Fluor 647 (AF647). However, while testing its compatibility with dSTORM imaging of neurofilament light chain (NfL), we noticed an unexpected loss of AF647 fluorescent signal in Vectashield. A quantitative analysis shows that there is an intensity drop to about 15% of the initial AF647 intensity in phosphate-buffered saline (PBS). Interestingly, lost AF647 signal can be partially recovered after washing. On the contrary, for Alexa Fluor 488, we saw an increase in intensity in Vectashield compared to PBS. Our results suggest that AF647 in Vectashield is not compatible with conventional fluorescence microscopy, because the dye gets quenched. Surprisingly, even though we can hardly identify positively labeled cells in Vectashield, we can still perform 3D dSTORM imaging of NfL. However, this is only possible by identifying labeled cells in PBS before adding Vectashield, i.e. before the images turn dark. Otherwise, it is not possible to tell apart background from a labeled cell. Our findings have important consequences not only for dSTORM, but for any type of fluorescence microscopy.

Introduction

Super-resolution microscopy (SRM) requires bright, densely labeled samples. Typical experiments start with dyes in a fluorescent state. This is necessary for the identification of labeled cells. A subsequent requirement for one type of SRM, dSTORM (direct stochastic optical reconstruction microscopy), is to get dye molecules to blink. Blinking separates individual fluorescent molecules in time and space. This enables their precise localization, which is necessary to reconstruct super-resolution diffraction-unlimited images[1,2]. In order to make them blink, dye molecules are switched to a dark state from which they stochastically and spontaneously recover to a fluorescent state, multiple times before bleaching. This can be achieved by special chemicals, such as thiol-containing reducing agents with or without enzymatic oxygen scavenger systems (e.g. GLOX buffer containing

glucose oxidase and catalase)[3,4]. It was recently reported that Vectashield, a commercial mounting medium, can also be used for dSTORM imaging of certain dyes, such as Alexa Fluor 647 (AF647)[5].

Results and discussion

In comparison with self-made buffers, commercially available Vectashield represent a very convenient and affordable choice for dSTORM imaging medium. The fact that it can be used off-the-shelf is especially important for demanding techniques such as dSTORM. Using the same imaging medium brings more reproducibility and allows for more comparable results within and between different laboratories. However, when we tried to use it for the imaging of neurofilament light chain (NfL), we noticed an unexpected loss of fluorescence in Vectashield compared to phosphate-buffered saline (PBS) (Fig. 1a,b). This is specific to AF647, as we do not see it with Alexa Fluor 488 (AF488; Fig. 2). To quantify fluorescence intensity changes we transfected the cells with NLS-mCherry plasmid. We chose to use NLS-mCherry for intensity measurements for multiple reasons. Firstly, it is uniformly distributed within the nucleus, and can be easily labeled with the same primary antibody, followed by either AF488- or AF647-conjugated secondary antibody. Additionally, mCherry gives a bright fluorescent signal in 561 channel that is not affected by any of the imaging media. This can be used for reliable identification of labeled regions of interest and intensity measurements of AF647 and AF488 before and after imaging media change (see material and methods for image acquisition and analysis details). A quantitative analysis shows there is an intensity drop to about 15 % of the initial value for AF647, and no loss of intensity for AF488 (Fig. 1d; Fig 3-4). Albeit not quantified before, this is in accordance with previously published work suggesting that Vectashield is not optimal for storing of AF647-labeled samples[6]. We first thought that our immunocytochemistry labeling with primary and secondary antibodies might not be stable. That is why we tested different types of AF647 stainings. We observed that the loss of fluorescence is not specific to our AF647-conjugated secondary antibody. We also see it for the cells labeled with an AF647-conjugated primary antibody (Figure 5) or AF647-phalloidin (Figure 6). However, AF647 quenching is more or less noticeable when looking at different cellular structures, probably depending on the starting labeling intensity. For example, tubulin immunocytochemistry still shows relatively nicely labeled cells in Vectashield (Fig. 5). Without seeing the image in PBS (before the addition of Vectashield), one might not even realize that there was quenching. That might be a reason why the AF647 quenching has not been reported before. On the other hand, even when we adjusted the image display (brightness/contrast) to show very dim pixel values (auto scale lookup table; Fig. 1c, inset), NfL shows hardly any signal and the labeling quality seems to be very poor. However, to our surprise, even with such “dark” NfL samples, it is still possible to do dSTORM. Although we can hardly identify positively labeled cells in Vectashield, we can still see blinking, perform 3D dSTORM imaging and even obtain SRM images with

a resolution of less than 40 nm (Fig. 1c), as estimated by Fourier ring correlation[7]. However, this was only made possible by identifying the labeled cell in PBS before adding Vectashield, i.e. before the image turned dark. Otherwise, it is not possible to tell apart background from a labeled cell. In addition to checking the cells in PBS first, and then switching to Vectashield for dSTORM, an alternative would be to use 25% Vectashield (Fig. 1d). It was previously reported that using 25% Vectashield in Tris-glycerol helps with reducing Vectashield's autofluorescent background[5]. Our quantitative analysis shows that 25% Vectashield does not induce quenching of AF647, similar to GLOX (Fig. 1d; Fig. 7). In the context of SRM imaging, this is very important, since it not only allows us to identify labeled cells, but also to evaluate the labeling quality, which is a prerequisite for successful dSTORM. While trying to understand the mechanism behind the quenching, we came across reports on Vectashield inducing cleavage of cyanine dyes and their derivatives (especially Cy2). We thought that this might be happening with AF647. We tested this hypothesis in a recovery experiment where we washed away Vectashield and after some time imaged the cells again in PBS. A quantitative analysis shows that the loss of AF647 is reversible since it can be partially recovered (Fig. 1d; Fig. 8; see material and methods for analysis details). The recovery would not have been possible if the dye was cleaved. In summary, we show that Vectashield induces quenching of AF647. On the contrary, AF488 fluorescence is increased in both pure and 25% Vectashield (respectively to 125 % and 185 % of the initial PBS values). Our findings have important consequences for any type of fluorescence microscopy. AF647 in Vectashield is not compatible with conventional fluorescence microscopy, because it gets quenched. This is especially of relevance for immunohistochemical stainings since Vectashield is used very commonly to mount tissue sections. Surprisingly, Vectashield-induced quenching does not hinder at least one type of microscopy, i.e. dSTORM. However, without knowing this, non-labeled and quenched cells cannot be distinguished. This would result in scientists not even trying to perform dSTORM, which would be wrong, considering the high quality of dSTORM images that can be achieved with Vectashield. Applying 3D dSTORM, we managed to obtain a super-resolution image of a neurofilament light chain in ND7/23 neuronal cell line. This type of imaging will open new opportunities for studying neurofilament organization in neuronal cells. This is important not only because of the structural role of neurofilaments, but also because of their recently discovered function as prognostic and diagnostic biomarkers in many neurological diseases.

Figures

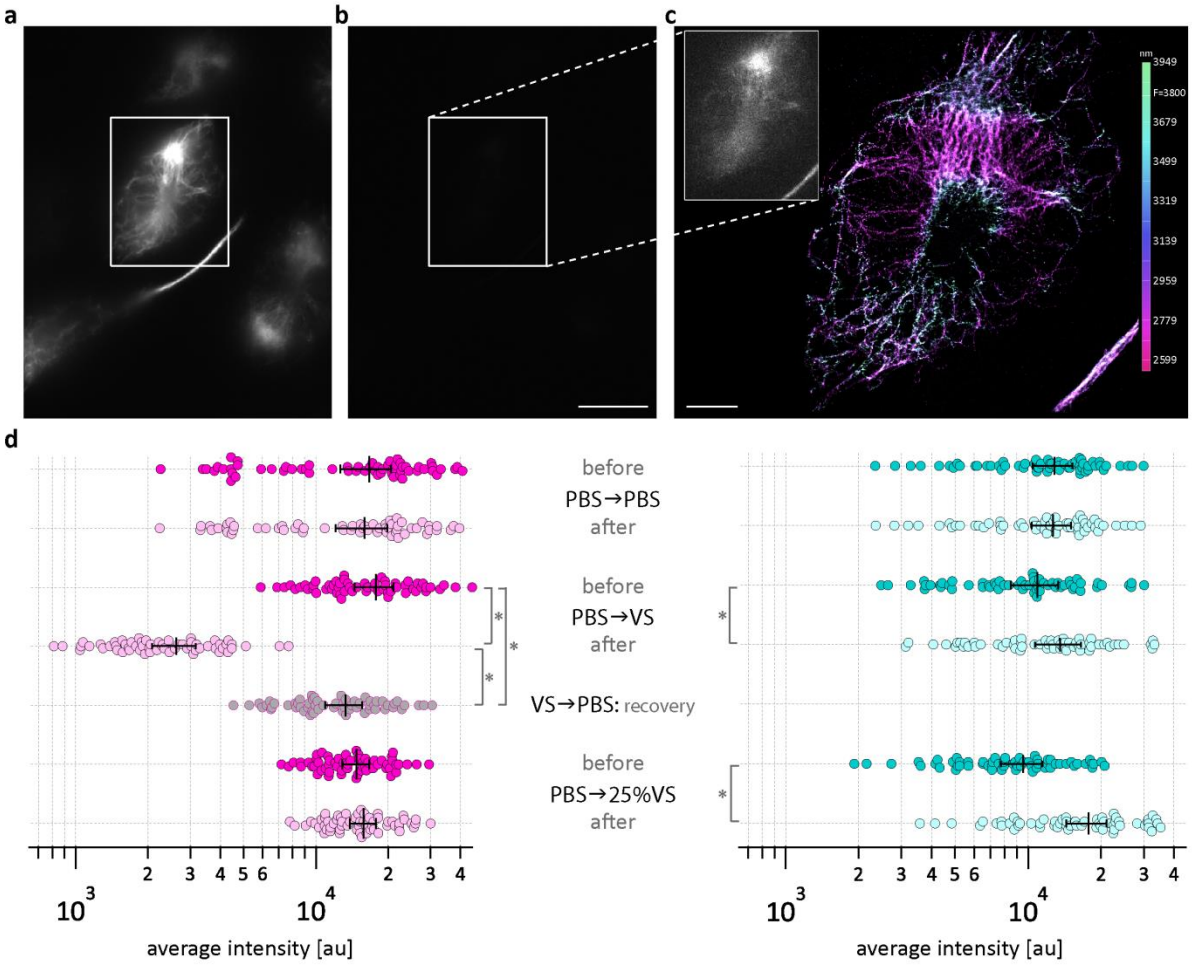

Figure 1. Vectashield (VS) quenches AF647 fluorescence, but does not hinder dSTORM imaging. ND7/23 cells were labeled with anti-NfL antibody, followed by AF647-conjugated secondary antibody (a-c). Cells were first imaged in PBS (a), then in Vectashield (b). After replacing PBS with Vectashield, there is a significant drop in AF647 fluorescence intensity. Boxed regions (a,b) show the location of the same cell. Brightness and contrast are linearly adjusted to show the same display range, so that the effects of two imaging media can be compared. Even with auto scale look up table (c, inset), one can hardly recognize the original cell. However, despite AF647 being quenched, the cell can still be successfully imaged with 3D dSTORM (c). The z positions in the dSTORM image are color-coded according to the height map shown on right. Quantification of intensity changes in different imaging media (PBS, VS, 25%VS) for AF647 (magenta) and AF488 (cyan) (d). NLS-mCherry transfected cells were labeled with anti-tRFP antibody, followed by AF647 or AF488-conjugated secondary antibody. In each case, cells were first imaged in PBS (before), followed by medium change (after). Average fluorescence intensity values of all images from 3 experiments (20 images per medium were analyzed in each experiment) are shown in the dot plot, including mean, and the standard error of the mean.

Post-hoc Bonferroni comparisons (more details in Supplementary material) show that in all 3 experiments there is a significant decrease of AF647 intensity after changing the medium from PBS to Vectashield (PBS→VS; $p<0.05$), as well as significant increase after washing (VS→PBS: recovery; $p<0.05$). For AF488, there is a significant increase of intensity in VS or 25%VS (PBS→VS, $p<0.05$; PBS→25% VS, $p<0.05$). Average intensity (X-axis) is shown on a logarithmic scale. Scale bars: a-b (20 μm), c (5 μm).

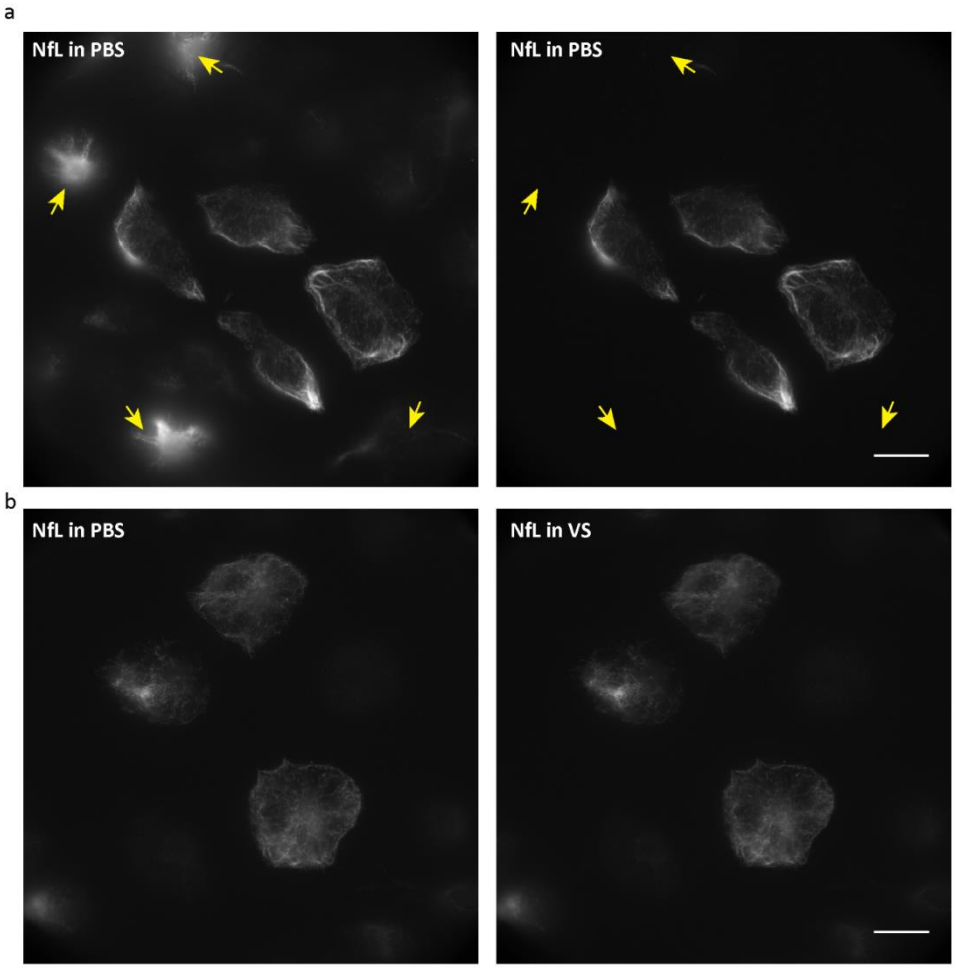

Figure 2. Comparison of PBS vs. Vectashield effect on AF488-labeled neurofilaments. ND7/23 cells labeled with anti-NfL primary antibody, followed by Alexa Fluor 488-conjugated secondary antibody. Cells were first imaged in PBS. Afterwards, PBS was replaced with PBS (a) or Vectashield (b). Left panels show images in PBS (before medium change) and right panels show images after medium change - in PBS (a) or Vectashield (b). In both cases, medium change does not seem to affect AF488 fluorescence intensity. Please note that some cells get washed away during medium change – they cannot be identified in the image after medium change, and are marked with yellow arrows. Scale bar: 20 µm (a,b).

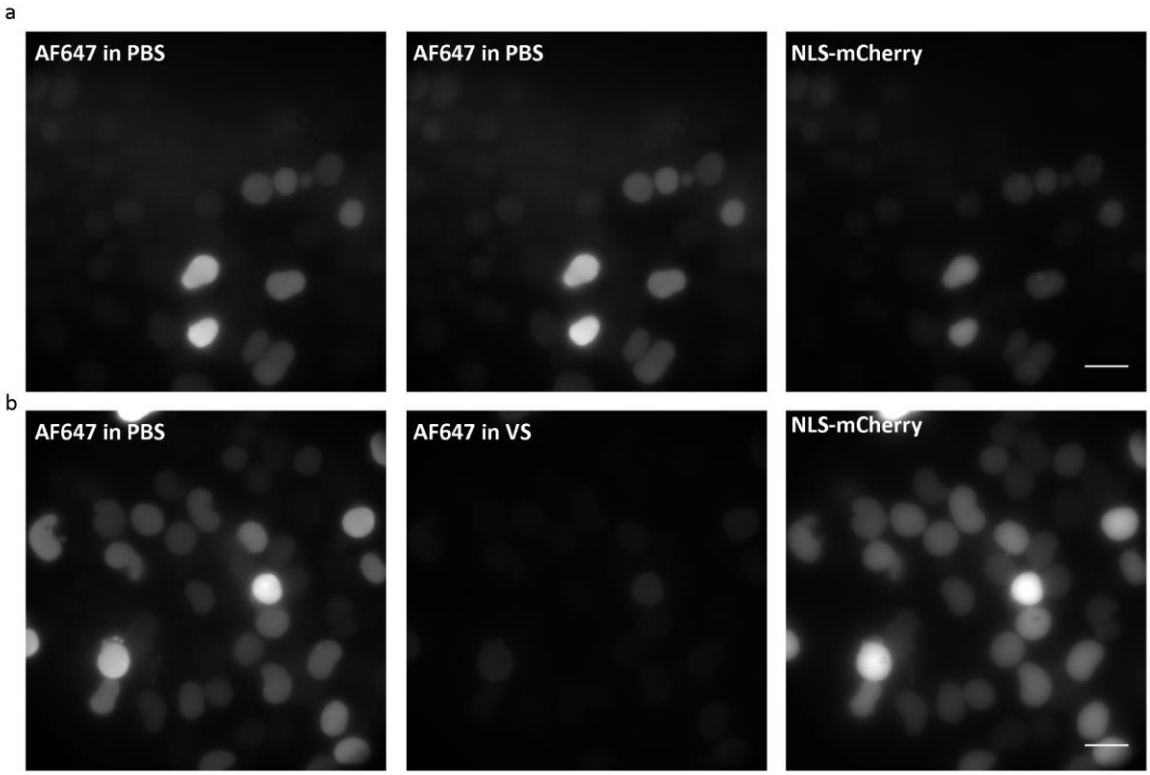

Figure 3. Comparison of PBS vs. Vectashield effect on AF647-labeled mCherry. ND7/23 cells expressing NLS-mCherry were labeled with anti-tRFP primary antibody, followed by AF647-conjugated secondary antibody. Cells were first imaged in PBS. Afterwards, PBS was replaced with PBS (a) or Vectashield (b). Left panels show images in PBS (before medium change) and middle panels show images after medium change - in PBS (a) there is no difference in AF647 intensity, while in Vectashield (b) there is a significant drop in the AF647 signal. Please note that these are two examples of images that were used for quantification of AF647 intensity changes in PBS vs. Vectashield (as shown in Figure 1d). Right panels show corresponding mCherry channel images after medium change. Scale bar: 20 µm (a,b).

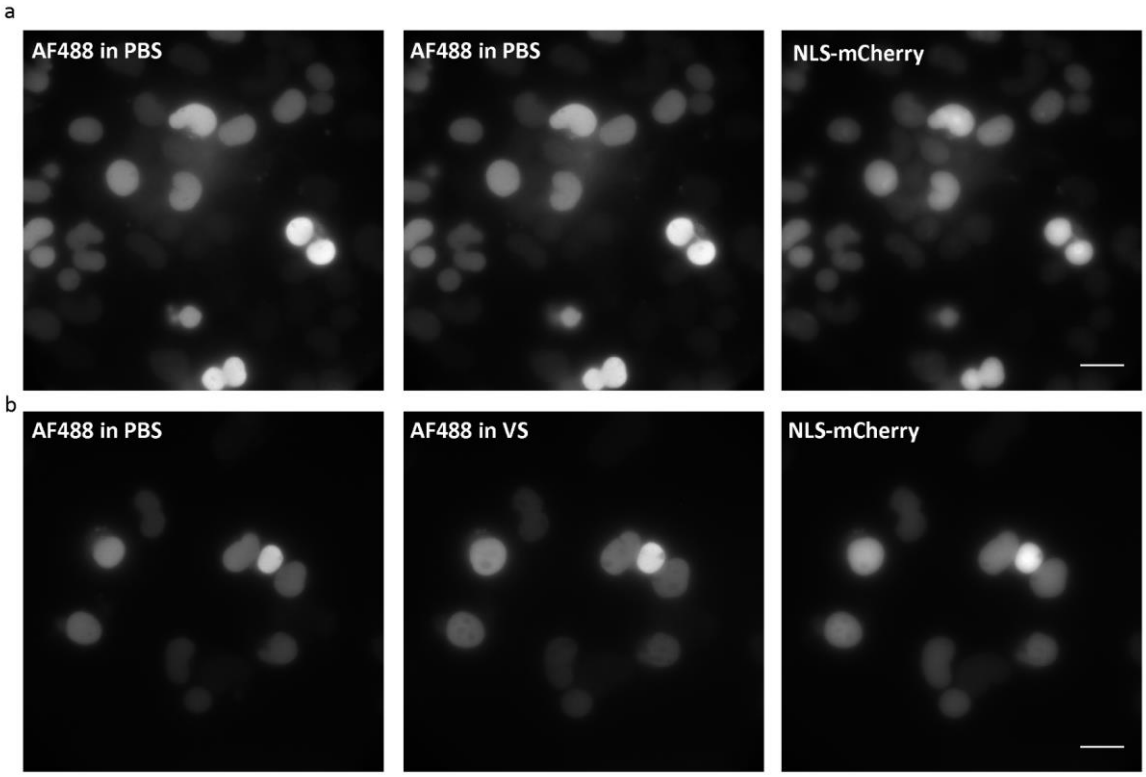

Figure 4. Comparison of PBS vs. Vectashield effect on AF488-labeled mCherry. ND7/23 cells expressing NLS-mCherry were labeled with anti-tRFP primary antibody, followed by AF488-conjugated secondary antibody. Cells were first imaged in PBS. Afterwards, PBS was replaced with PBS (a) or Vectashield (b). Left panels show images in PBS (before medium change) and middle panels show images after medium change - in PBS (a) or Vectashield (b). In contrast to AF647 (Supplementary Figure 2), Vectashield does not quench AF488 fluorescence. Please note that these are two examples of images that were used for quantification of AF488 intensity changes in PBS vs. Vectashield (as shown in Figure 1d). Right panels show corresponding mCherry channel images after medium change. Scale bar: 20 µm (a,b).

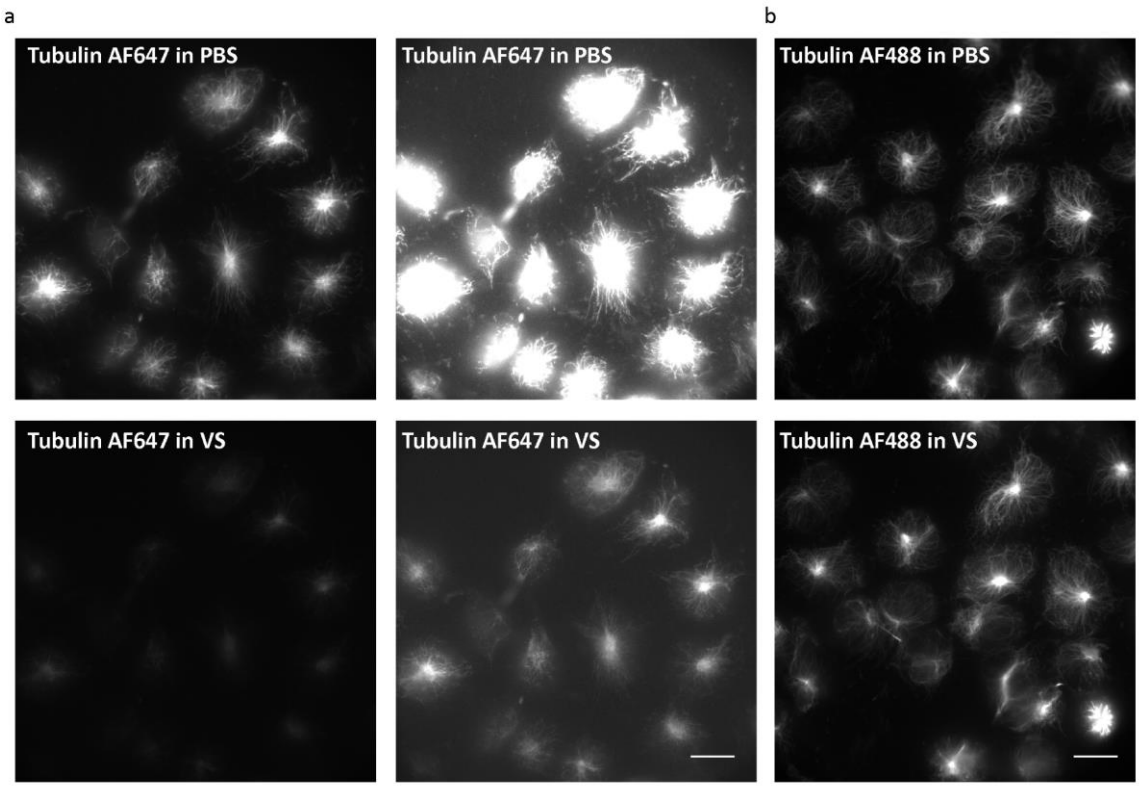

Figure 5. Vectashield effect on AF647- vs. AF488-labeled microtubules. ND7/23 cells labeled with AF647- (a) or AF488-conjugated (b) anti-Tubulin β3 (TUBB3) antibody. Cells were first imaged in PBS (upper panels). Afterwards, PBS was replaced with Vectashield (lower pannels). As shown in the panel (a), after replacing PBS with Vectashield, there is a drop in the AF647 fluorescence intensity. Please note that left and middle panels in (a) show the same images for which brightness and contrast levels were adjusted differently in order to make the quenched AF647 signal in Vectashield visible. In contrast to AF647, Vectashield does not quench AF488 fluorescence (b). Scale bar: 20 µm (a,b).

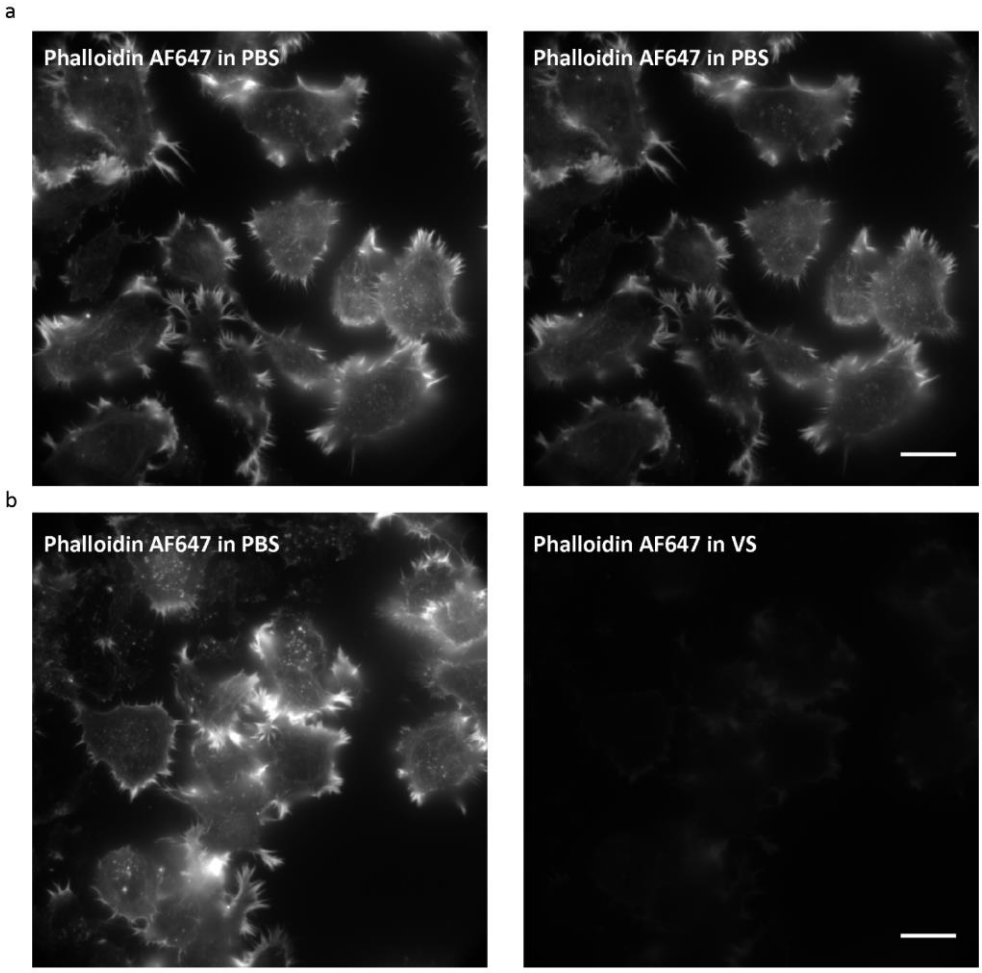

Figure 6. Comparison of PBS vs. Vectashield effect on AF647-phalloidin. ND7/23 cells were labeled with phalloidin Alexa Fluor 647. Cells were first imaged in PBS. Afterwards, PBS was replaced with PBS (a) or Vectashield (b). Left panels show images in PBS (before medium change) and right panels show images after medium change - in PBS (a) there is no difference in AF647 intensity, while in Vectashield (b) there is a drop in the AF647 signal. Scale bar: 20 µm (a,b).

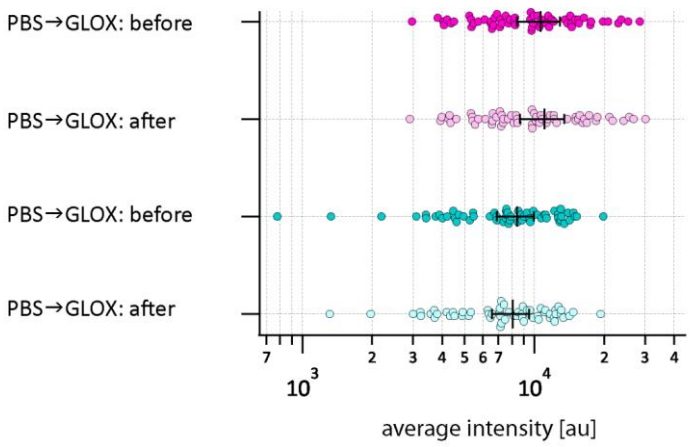

Figure 7: Analysis of AF647 and AF488 fluorescence intensity changes in GLOX buffer. ND7/23 cells expressing NLS-mCherry were labeled with anti-tRFP primary antibody, followed by AF647- or AF488-conjugated secondary antibody. Cells were first imaged in PBS. Afterwards, PBS was replaced with GLOX. Fluorescence intensity measurements were done in images taken before and after PBS to GLOX (PBS→GLOX) change. Quantification is done as in Fig. 1d. For each condition (PBS→GLOX: before; PBS→GLOX:after; AF647 is shown in magenta; AF488 in cyan), average fluorescence from individual images from all 3 experiments (20 images per experiment per medium were analyzed; total of 60) is shown in the graph, including the mean for all 60 data points, and standard error of the mean. Post-hoc Bonferroni comparisons (more details in Supplementary material) show that in all 3 experiments for both AF488 and AF647 there is no significant intensity change after switching the imaging medium from PBS to GLOX. Average intensity (X-axis) is shown on a logarithmic scale.

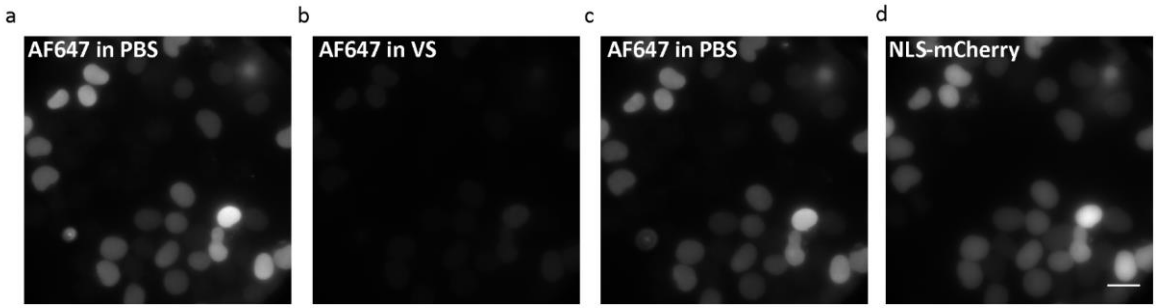

Figure 8: Recovery of AF647 fluorescence after removal of Vestashield. ND7/23 cells expressing NLS-mCherry were labeled with anti-tRFP primary antibody, followed by AF647-conjugated secondary antibody. Cells were first imaged in PBS (a), then in Vectashield (b). Afterwards, Vectashield was replaced with PBS, cells were washed and imaged 2.5 h later in PBS (c). After medium change - in Vectashield (b) there is a significant drop in the AF647 fluorescence intensity that is partially recovered after washing in PBS (c). Please note that this is example of an image that was used for quantification of AF647 intensity changes after recovery (as shown in Figure 1d). mCherry channel image corresponding to panel (c) is shown in (d). Scale bar: 20 µm (a-d).

Material and methods

Cell culture

Mouse neuroblastoma x rat neuron hybrid ND7/23 cells (ECACC 92090903, obtained from Sigma Aldrich) were grown in high glucose Dulbecco's Modified Eagle Medium (DMEM; Thermo Fisher Scientific, cat. no. 41965062) supplemented with 10 % heat-inactivated fetal bovine serum (FBS; Thermo Fisher Scientific, cat. no. 10270106), 1 % penicillin-streptomycin (Sigma Aldrich, cat. no. P0781), 1 % sodium pyruvate (Thermo Fisher Scientific, cat. no. 11360039) and 1 % L-glutamine (Thermo Fisher Scientific, cat. no. 25030024) at 37 °C, 5 % CO_2. FBS was heat-inactivated by incubation at 56 °C for 30 minutes. Cells were passaged every 2-3 days up to passage 18-20 and were not differentiated.

For all the experiments, cells were seeded on a four-well Lab-Tek II chambered #1.5 German coverglass (Thermo Fisher Scientific, cat. no. 155382), 70,000 cells per well. Lab-Teks were coated with poly-D-lysine (Sigma Aldrich, cat. no. P6407) diluted in ddH2O at a 1 µg/ml concentration, and incubated at least 4 h at room temperature (RT). Before seeding wells were washed twice with Dulbecco's phosphate-buffered saline (DPBS; Thermo Fisher Scientific, cat. no. 14190169) or ddH_2O and left in the hood to dry completely.

Constructs and cloning

NLS (nuclear localization sequence)-mCherry construct was made by inserting NLS-mCherry sequence into a commercially available pcDNA™3.1/Zeo(+)mammalian expression vector (Invitrogen). NLS sequence was added upstream of the mCherry gene (gift from Edward Lemke's laboratory, EMBL, Heidelberg) by polymerase chain reaction (PCR). The following primers were used for cloning: 5'-GCTGGCGCTAGCACCATG**CCGCCGAAAAAAAAACGCAAAGTGGAAGATAGC**GTGAGCAAGGGCGAGGAGG-3' (forward primer with NheI restriction site; NLS sequence is shown in bold) and 5'-CGCGCAGCGGCCGCTCACTTGTACAGCTCGTCCATGCCG-3' (reverse primer with NotI restriction site). Generated plasmid sequence was confirmed by sequencing.

Transfections (for AF647 and AF488 intensity measurements)

For Alexa Fluor 647 (AF647) and Alexa Fluor 488 (AF488) intensity measurement experiments, ND7/23 cells were transfected with NLS-mCherry plasmid. Cells were transfected using JetPrime (Polyplus-transfection, cat. no. 114-15) one day after seeding, at 80-85 % confluence, according to

the manufacturer´s instructions. On the following day, NLS-mCherry expression was confirmed on an epifluorescent inverted microscope (Olympus CKX41) and immunostaining was started.

Immunocytochemistry stainings

For immunostaining of NLS-mCherry, cells were washed briefly with 0.01 M phosphate-buffered saline (PBS; 137 mM NaCl, 10 mM Na_2HPO_4, 1.8 mM KH_2PO_4, 2.7 mM KCl, pH 7.4) and fixed with 2 % paraformaldehyde (PFA; Sigma Aldrich, cat. no. 158127) in PBS for 10 min at RT. After fixation, cells were briefly washed 3 times, blocked and permeabilized with 10 % goat serum (GS; Thermo Fisher Scientific, cat. no. 16210064)/0.5 % Triton X-100/PBS (Sigma Aldrich, cat. no. X100) for 1 h. NLS-mCherry was stained with rabbit anti-tRFP (turbo red fluorescent protein) antibody (Evrogene, cat. no. AB233) diluted 1:500 in 5 % GS/0.1 % Triton X-100/PBS. The cells were incubated with primary antibody at least 18 h at 4 °C. On the following day, cells were washed 3 times (5 minutes each wash) and incubated with secondary goat anti-rabbit antibody conjugated with either AF647 (Thermo Fisher Scientific, cat. no. A-21245) or AF488 (Thermo Fisher Scientific, cat. no. A-11034) for 1 h at RT. Secondary antibodies were diluted 1:500 in 5 % GS/0.1 % Triton X-100/PBS. After incubation with the secondary antibody, cells were washed 3 times (5 minutes each wash) and incubated in PBS until imaging. All the washing steps were performed with PBS. Imaging was performed on the same or following day.

For immunostaining of neurofilament light chain (NfL), cells were rinsed briefly with Tris-buffered saline (TBS; 20 mM Tris, 150 mM NaCl, pH 7.6) and then fixed with 2 % PFA for 15 minutes at RT. After fixation, cells were washed three times (5 minutes each wash) with TBS and blocked in 3 % GS/0.3 % Triton X-100/TBS for 40 minutes at RT. Cells were incubated with mouse anti-neurofilament 70 kDa antibody, clone DA2 (Merck Millipore, cat. no. MAB1615) diluted 1:250 in 1 % GS/0.3 % Triton X-100/TBS for 2.5 h at RT, followed by overnight incubation at 4 °C. On the following day, cells were washed 3 times (5 minutes each wash) with TBS, and incubated with goat anti-mouse secondary antibodies conjugated with AF647 (Thermo Fisher Scientific, cat. no. A32728) or AF488 (Thermo Fisher Scientific, cat. no. A32723) for 1 h at RT. Secondary antibodies were diluted 1:500 in 1 % GS/0.3 % Triton X-100/TBS. Afterwards, cells were washed 3 times (5 minutes each wash) with TBS. TBS was used instead of PBS for this immunostaining because of potential influence of PBS on phosphorylated neurofilaments. Only before imaging, TBS was replaced with PBS. Imaging was performed on the same day.

For actin labeling with phalloidin AF647, cells were rinsed briefly with PBS and fixed with 2 % PFA, for 15 minutes at RT. After fixation, cells were washed 3 times briefly with PBS and blocked 1.5 h at RT in 5 % bovine serum albumin (BSA; Sigma Aldrich, cat. no. A9647) diluted in 0.3 % Triton X-100/PBS.

After blocking, cells were incubated with 0.25 µM AF647 phalloidin (Thermo Fisher Scientific, cat. no. A22287) diluted in PBS, ON at 4 °C. On the following day, cells were incubated in AF647 phalloidin for additional 4 h at RT and subsequently washed 3 times (5 minutes each wash) with PBS. Imaging was performed on the same day.

For tubulin labeling cells were fixed as described previously[5]. Briefly, the cells were first washed with PBS and extracted in 0.5 % Triton X-100 diluted in microtubule stabilization buffer (MTSB; 80 mM PIPES, 1 mM $MgCl_2$, 5 mM EGTA, pH 6.8) for 10 seconds. Cells were washed once briefly with PBS, and fixed in -20 °C methanol for 10 minutes at -20 °C. Afterwards, cells were washed 3 times (10 minutes each wash) and blocked for 1 h at RT in 5 % BSA/PBS. Cells were incubated with AF647 anti-Tubulin β3 (TUBB3) antibody (BioLegend, cat. no. 801210) or AF488 anti-Tubulin β3 (TUBB3) antibody (BioLegend, cat. no. 801203) diluted 1:100 in 5 % BSA/PBS, 3 h at RT. Afterwards, cells were washed 3 times (5 minutes each wash) with PBS and imaged on the same day. All washing, incubation and blocking steps were performed on the shaker.

Imaging of tRFP labeled cells (for AF647 and AF488 intensity measurements)

Imaging of tRFP labeled cells was performed on an inverted Nikon microscope (Nikon Instruments), equipped with XY-motorized stage, Perfect Focus System and N-STORM module, all controlled by NIS-Elements AR software (Nikon Instruments). The images were acquired using an oil-immersion objective (HP Apo TIRF 100×H, NA 1.49, Oil), in epifluorescent widefield mode, with 10 ms exposure time, 1024x1024 pixels frame size and 16-bit image depth. Following filter cubes were used: 488 (AHF; EX 482/18; DM R488; BA 525/45), 561 (AHF; EX 561/14; DM R561; BA 609/54) and Cy5 (AHF; EX 628/40; DM660; BA 692/40). Filtered emitted light was imaged with ORCA-Flash 4.0 sCMOS camera (Hamamatsu Photonics).

tRFP labeled cells were first briefly checked in PBS using brightfield illumination. For each well in the Lab-Tek we did following: picked randomly 30 fields of view (stage positions) using brightfield illumination, saved xyz coordinates of each field of view in NIS-Elements AR software and acquired images automatically by using NIS-Elements ND multipoint acquisition module, which allowed us to go to the same position each time. To provide that the cells were always properly focused, we used an autofocusing function of ND multipoint acquisition module.

Imaging was done first in PBS, using 561 (mCherry channel) and either 488 (AF488 channel) or Cy5 (AF647 channel) filter cube, depending on the labeling condition. Excitation light intensity for mCherry and AF647 channels was 10 % and for AF488 channel 5 %. Afterwards, PBS was replaced with one of the following imaging media: PBS, 100 % Vectashield (VS; Biozol, cat. no. VEC-H-1000), 25 % Vectashield or GLOX. We made 25 % Vectashield by mixing VS with Tris-Glycerol in 1:4 v/v ratio.

Tris-glycerol was obtained by adding 5 % v/v 1 M Tris, pH 8 to glycerol (Sigma Aldrich, cat. no. G2025). For preparation of GLOX buffer, we used Buffer A (10 mM Tris, pH 8, 50 mM NaCl), Buffer B (50 mM Tris, pH 8, 10 mM NaCl) and GLOX solution. GLOX solution was made by mixing 14 mg glucose oxidase (Sigma Aldrich, cat. no. G2133), 50 µl catalase (17 mg/ml; Sigma Aldrich, cat. no. C3155) and 200 µl Buffer A. Aliquots of GLOX solution were kept at -20 °C. GLOX buffer was prepared fresh, prior to use by mixing 7 µl GLOX solution with 690 µl Buffer B containing 10 % w/v glucose (Sigma Aldrich, cat. no. D9559) on ice. For AF647 recovery experiments, 100 % Vectashield was removed and cells were washed twice with PBS. After 2.5 h, cells were washed one more time with PBS and imaging was repeated. To provide enough data for analysis each experiment was repeated at least three times for AF488 labeled cells and AF647 labeled cells.

Imaging of actin (phalloidin) and tubulin labeled cells

Phalloidin AF647 labeled cells were first checked in PBS, using fluorescent light source (Lumencor Sola SE II) and Cy5 filter cube with 10 ms exposure time and 5 % excitation light intensity. Up to 40 fields of view (positions) per well were picked and xyz coordinates of each field of view were saved in NIS-Elements AR software. Widefield image acquisition was then performed automatically by using NIS-Elements ND multipoint acquisition module at 30 ms exposure time and 10 % of fluorescent light source. Both, brightfield and fluorescence images were acquired. Afterwards, PBS was replaced with Vectashield, left 2 minutes to completely cover the sample and acquisition was repeated. Upon the addition of Vectashield we noticed a change in focus, so before acquiring images in Vectashield, every field of view needed to be manually refocused. During the imaging, autoscaling look-up table (LUT) was on, which allowed us to see what would approximately be the correct focus plane, despite the quenching of fluorescent signal.

Tubulin AF647 or AF488 labeled cells were imaged by following the same procedure as described above, using Cy5 filter cube (AF647) or 488 filter cube (AF488).

3D dSTORM imaging of NfL

3D dSTORM (direct stochastic optical reconstruction microscopy) imaging was performed by using the N-STORM module of the same microscope, as described above. For imaging, oil-immersion objective (HP Apo TIRF 100×H, NA 1.49, Oil) and 647 nm laser (LU-NV Series Laser Unit) were used. Fluorescent light was filtered through a Cy5 filter cube. Filtered emitted light was imaged with ORCA-Flash 4.0 sCMOS camera (Hamamatsu Photonics) with cylindrical lens introduced in the light path[8].

Fluorescent and brightfield images of NfL labeled cells in PBS and Vectashield were acquired following the same procedure that was used for imaging of phalloidin AF647 labeled cells, as

described above. After widefield acquisition, selected fields of view were imaged with 3D dSTORM. Imaging was performed in total internal reflection fluorescence (TIRF) mode with continuous 647 nm laser illumination (full power). Frame size was 256x256 pixels and image depth 16-bit. For each 3D dSTORM image, 30,000 frames were acquired at 33 Hz.

Calibration of 3D dSTORM was done previously using TetraSpeck Microspheres (Thermo Fisher Scientific, cat. no. T7279) following NIS-Elements' instructions. 3D dSTORM image processing was performed in NIS-Elements AR software. Molecule identification settings were set to defaults for 3D dSTORM analysis: minimum width 200 nm, maximum width 700 nm, initial fit width 300 nm, max axial ratio 2.5 and max displacement 1. Minimum height for peak detection was set to 200, and localization analysis was performed with overlapping peaks algorithm. Resulting molecule lists were exported as text files and analyzed by Fourier ring correlation (FRC)[7] to determine the image resolution. Based on FRC resolution estimate (35-40 nm), we reconstructed 3D dSTORM images with Gaussian rendering size of 15 nm in NIS Elements AR. Brightness and contrast were adjusted with Gaussian rendering intensity and height map with color coded molecule height (z location) was added. Final 3D dSTORM image was then exported as a tiff image. Z rejected molecules were excluded from resolution analysis and from final images.

Image analysis and intensity measurements

Intensity measurements for quantitative analysis of AF647 and AF488 were done in Fiji/ImageJ[9]. Images in ND2 format were opened using Bio-Formats plugin[10] and converted to tiff before the analysis. Original bit depth (16-bit) was used for analysis. For presentation purposes, brightness and contrast of 16-bit images were linearly adjusted in Fiji, images were converted to 8-bit and imported in Adobe Illustrator.

In all of our experiments (except recovery of AF647) each field of view was imaged two times: in 561 (mCherry) and either 647 (AF647) or 488 (AF488) channel, before and after medium change. As result, for each field of view we had four fluorescent pictures, mCherry and AF647(or AF488) before and after medium change. In AF647 fluorescence recovery experiments each field of view was imaged three times: in mCherry and AF647 channel, before medium change, after changing to Vectashield and after washing in PBS. Consequently, for each field of view in recovery experiments we had six fluorescent pictures, mCherry and AF647 before medium change, in Vectashield and after washing in PBS.

For the purpose of analysis, we made a macro that allowed us to stack and align all images of each field of view and perform the intensity measurements in same regions of interest (ROIs). Images from

mCherry channel were used for alignment and thresholding, while intensity measurements were done in images from AF647 and AF488 channels, respectively.

Macro was designed to open and stack images from mCherry channel, align them using MultiStackReg (developed by Brad Busse http://bradbusse.net/sciencedownloads.html) and TurboReg plugin[11], and save the alignment information in a form of transformation matrices. After that, macro was opening and stacking images from AF647 channel. AF647 images were aligned using transformation matrices that were saved after alignment of mCherry images. This way we ensured that images from 647 channel would be properly aligned even in the case when one of them has very low intensity (e.g. images taken in Vectashield). After alignment both mCherry and AF647 image stacks were cropped to exclude empty space. Same procedure was done for AF488 images.

Region of interest for intensity measurements was created by thresholding in mCherry image stack, using Otsu Dark thresholding algorithm. Thresholding was performed in the image that was taken after medium change to exclude cells that were washed away during the change of imaging media. Resulting ROI contained fluorescently labeled nuclei and we refer to it as nuclear ROI. At this point, user intervention was required, to choose ROI that contains no cells, only background noise (background ROI). Afterwards, intensity measurements (mean intensity and integrated density) of nuclear and background ROIs were performed in AF647 and AF488 stacks, respectively.

As a result of analysis, macro saved intensity measurement results (in a form of a text file), mCherry before/after image stacks, AF488 or AF647 before/after image stacks and nuclear ROIs. Oversaturated images, poorly aligned images and images where all cells were washed away during imaging media change were excluded from further analysis.

Text files with intensity measurement results were imported in Excel and corrected total cell fluorescence (CTCF) was calculated.

CTCF = Integrated Density of nuclear ROI – (area of nuclear ROI x mean fluorescence of the background)

In addition to CTCF, we calculated average fluorescence by dividing CTCF with the area of nuclear ROI. Calculated values were exported to a separate Excel file for statistical analysis.

Statistical analysis

Statistical analyses (ANOVA and post-hoc analyses) were carried out with IBM SPSS Statistics Version 25, Armonk, New York, USA. The power analysis to determine the optimal sample size was carried

out with the Statistical Tree Power Calculator, QFAB (Queensland Facility for Advanced Bioinformatics), Brisbane, Australia.

Preparation of data analysis based on pilot work

The dependent variable was the difference (delta) between the fluorescence intensities before and after media change, where the starting medium is always PBS and the change is represented by removing PBS and adding another medium (delta intensity = (intensity PBS – intensity new medium)). Based on prior assumptions, this difference will become minimal in the control condition, where PBS is first removed and the added new medium is again PBS. If another medium is added, delta will be larger and take on an either positive or negative value, depending on whether the intensity in the new medium is smaller or larger than the intensity of PBS.

The dependent variable (delta intensity) delivers continuous values and is on interval scale level, which is a prerequisite to carry out an analysis of variance (ANOVA). The independent variables (factors) were different dyes (AF647 and AF488), different imaging media (PBS, Vectashield, 25% Vectashield, GLOX) and different experiments (1, 2 and 3).

Power calculations, randomization and design

Prior to the actual experiments, it was necessary to carry out power calculations to specify the optimal sample size. These analyses needed to take into account multiple analyses, including the different experiments and post-hoc comparisons. Our main focus was to compare delta intensities between different imaging media applying ANOVA. Our defined type 1 error level was 0.05 (including two sided testing for post-hoc, planned comparisons). We aimed for a power of 0.95 (which equals a type 2 error level of 0.05). Based on pilot work, we had estimated to find at least an effect size between 0.45 and 0.5 and more realistic an effect size between 0.8 and 0.9. For the lowest effect of 0.45 we would need 23 measurements per condition, for the large effect size of 0.9 we would only need 7 measurements per group to reach the pre-specified power of 0.95. To fulfil the assumptions of ANOVA and post-hoc tests in terms of required distributions, we decided for 20 measurements per condition, which lies within the range of 7 to 23 measurements. We decided in favor of a value at the upper limit of this range because the smaller the sample size, the more likely are violations to the assumptions of parametric tests such as ANOVA. We did not go beyond this range, though, to avoid having over-powered statistical tests, where tiniest differences would become statistically significant. In our pilot work, we also realized that if images are taken truly at random, a minority of the images could not be measured because no cells appeared after changing media (they got washed away), or some of the images were oversaturated. Because randomization was an absolute requirement for our statistical tests, we needed to have a bigger number than 20 images randomly taken to get a

total of 20 measurements. To be safe, we decided a priori that 30 images are taken at random and the first 20 valid images (i.e. those that contained cells before and after media change and that did not contain oversaturated pixels) were included in the analysis. The remaining images were not considered in the analysis. This resulted in the following design:

In each experiment, 20 delta intensities were measured for all 4 different imaging media (20 * 4 = 80). Because they were measured for both dyes, AF647 and AF488, there were 160 delta intensities (80 * 2) per experiment. Because we carried out 3 experiments, there were 480 delta intensities in total (160 * 3).

As a result, there was a 2 (dye) * 4 (imaging media) * 3 (experiment) ANOVA on delta intensities. Following our a priori assumptions, we assumed the two dyes would deliver different delta intensities. In addition, we assumed the 4 imaging media would differ in terms of their delta intensities. Because each experiment took place on a different day with new cells (that were freshly transfected and labeled, etc.), we also expected that the 3 experiments would differ in terms of their delta intensities. In case the 3 experiments indeed differ, different ANOVAs are necessary for each experiment separately, in order to show that the differences between the imaging media point in the same direction and the same post-hoc comparisons are significant in each individual experiment. In these individual ANOVAs, the delta intensities for all imaging media are directly compared to each other for each experiment separately and for each dye separately. Planned post-hoc comparisons (Bonferroni) are subsequently carried out to demonstrate that all post-hoc analyses show the same type of significant differences between the compared imaging media. These planned comparisons correct the significance levels for multiple tests, i.e. they avoid an accumulation of statistical error which would otherwise occur if multiple significance tests were carried out. To give us maximum trust in our results, we chose the strictest of all post-hoc comparisons, which is the Bonferroni correction. Bonferroni delivers the most conservative results, i.e. the least likely to become statistically significant.

Deriving hypotheses based on prior observations

Based on pilot experiments, our primary focus was dye AF647, because only in AF647 we noticed an intensity drop in image medium Vectashield compared to PBS. We expected that this drop was shown in all 3 experiments. We did not expect such a drop for dye AF488. We do, however, also expect intensity changes on other imaging media for dye AF488. Based on pilot work, we expected medium sized effects relating to a delta intensity increase for Vectashield and 25 % Vectashield. If this increase is robust, it should appear in all three experiments.This also requires planned post-hoc

comparisons (Bonferroni), to demonstrate that the significant differences between the compared imaging media are the same for all 3 experiments.

Based on pilot data, we had yet another hypothesis. We realized an intensity drop seen for dye AF647 after adding Vectashield and found out that the intensity will recover after washing. This would be in contrast to the previously assumed dye cleavage effect, where no recovery would be expected. In order to test whether the AF647 intensity drop seen in Vectashield can actually recover, we carried out a repeated measurement ANOVA. In this ANOVA, we compared 3 intensities (1. at PBS baseline, 2. after removing PBS and adding Vectashield, 3. after replacing Vectashield with PBS and waiting 2.5 hours in PBS imaging medium).

Data analyses

In a first step, we carried out a 2 (dye) * 4 (imaging media) * 3 (experiment) ANOVA with the dependent variable delta intensities. There was a significant main effect for dye, $F(1, 456)=819.14$, $p<0.001$, effect size partial $\eta^2=0.64$, Mean AF647=3596.45, Mean AF488=-2569.74, SE(Means)=152.34. Similarly, there was a significant main effect for imaging media, $F(3, 456)=424.15$, $p<0.001$, effect size partial $\eta^2=0.74$, Mean PBS=420.74, Mean Vectashield=6239.29, Mean_25% Vectashield=-4583.83, Mean GLOX=-22.79, SE(Means)=215.45. In addition, there was a significant main effect for experiment, $F(2, 456)=17.58$, $p<0.001$, effect size partial $\eta^2=0.07$, Mean expt 1=864.28; Mean expt 2=-383.07; Mean expt 3=1058.85, SE(Means)=186.58. Finally, all possible combinations of interactions between the factors were significant, $p<0.001$. In summary, the delta intensity values differ between dyes, between imaging media, between experiments and the combination of these factors influence each other differently depending on the chosen combination. Consequently, this analysis including all possible factors and their combinations does not permit conclusions, calling for separate ANOVAs in each of the two dyes and separate ANOVAs in each of the 3 experiments. From a biological point of view, it would also not make sense to carry out one ANOVA across both dyes and all conditions.

Separate ANOVA for AF647 in each of the 3 experiments

For dye AF647, there was a main effect for imaging media in all 3 experiments, Experiment 1: $F(3, 76)=164.46$, $p<0.001$, effect size partial $\eta^2=0.87$; Experiment 2: $F(3, 76)=182.45$, $p<0.001$, effect size partial $\eta^2=0.88$; Experiment 3: $F(3, 76)=114.06$, $p<0.001$, effect size partial $\eta^2=82$. Looking at the planned, post-hoc comparisons (Bonferroni), the same result was shown in all three experiments: there was a significant ($p<0.05$) drop of delta intensity from PBS to Vectashield (PBS→VS): Experiment 1 mean delta intensity drop=19348.86, SE(mean intensity drop)=1150.76, Experiment 2 mean delta intensity drop=10163.16, SE(mean intensity drop)=564.35, Experiment 3 mean delta

intensity drop=13821.93, SE(mean intensity drop=975.89). The other media (25 % Vectashield and GLOX) did not differ significantly from PBS in all 3 experiments, i.e. there was no significant intensity drop. Consequently, the results in all 3 experiments support the notion of an intensity drop only from PBS to Vectashield. This was the result we had expected based on our pilot data. The results are robust because we did not rely on experiment 1 alone, but replicated the results in experiments 2 and 3. In all 3 experiments, exactly the same main effects were observed and exactly the same post-hoc comparisons reached statistical significance.

Analysis of AF647 recovery

In addition, we carried out a repeated measures ANOVA to test whether the intensity drop seen in Vectashield can actually recover. We had hypothesized this recovery based on earlier observations we had made in our laboratory when running pilot experiments. Now, we could not rely on delta intensities from 2 measurements, but were rather interested in intensities at 3 different time points. We compared three intensities (1. at PBS baseline, 2. after removing PBS and adding Vectashield, 3. after replacing Vectashield with PBS and waiting for 2.5 hours in PBS imaging medium). We again performed these comparisons for all three experiments separately. In this example, we had a repeated measurement with three consecutive measurements. In this case, the respective analysis depends on a prerequisite for a repeated measurements ANOVA: if sphericity can be assumed based on the Mauchly's Test of Sphericity, no corrections need to be performed. Otherwise, the Greenhouse-Geisser Test of an overall "within subjects effect" with corrected degrees of freedom has to be applied. Because the Mauchly's Test of Sphericity revealed a significant result for all three experiments ($p<0.001$), sphericity could not be assumed and the Greenhouse-Geisser Test was applied for all three experiments. In all three experiments, intensity differences between the 3 repeated conditions were statistically significant (1. PBS baseline, 2. after removing PBS and adding Vectashield, 3. after replacing Vectashield with PBS and waiting for 2.5 hours in PBS imaging medium), Experiment 1: $F(1.01, 19.26)=162.68$, $p<0.001$; effect size partial $\eta^2=0.895$; Experiment 2: $F(1.03, 19.48)=175.17$, $p<0.001$, effect size partial $\eta^2=0.9$; Experiment 3: $F(1.18, 22.38)=104.28$, $p<0.001$, effect size partial $\eta^2=0.85$. Given that all three experiments showed a significant overall effect for the repeated conditions, we carried out planned, post-hoc tests with Bonferroni correction to evaluate which of the three time points significantly differed from each other. In each of the three experiments, there was a significant intensity drop from 1. PBS baseline to 2. after removing PBS and adding Vectashield (PBS→VS; in each experiment, $p<0.05$). Similarly, there was a significant recovery from 2. after removing PBS and adding Vectashield to 3. After replacing Vectashield with PBS and waiting for 2.5 hours in PBS imaging medium (VS→PBS:recovery, in each experiment, $p<0.05$). In all three experiments, the recovery was never as strong as to reach the original intensity (in each

experiment, $p<0.05$). Consequently, the results demonstrating the recovery effect were very robust. The drop as well as the recovery effect was not only shown in Experiment 1, but replicated exactly in Experiments 2 and 3. In addition, all other post-hoc tests revealed the same results in all three experiments.

Detailed results are as follows:

Experiment 1 had a PBS baseline intensity mean=24036.37, SE(mean)=1928.87, a drop after removing PBS and adding Vectashield with a mean=3638.06, SE(mean)=359.85, and a recovery after replacing Vectashield with PBS and waiting for 2.5 hours with a mean=16554.7, SE(mean)=1394.89.

Experiment 2 had a PBS baseline intensity mean=12270.01, SE(mean)=921.22, a drop after removing PBS and adding Vectashield with a mean=1855.48, SE(mean)=151.16, and a recovery after replacing Vectashield with PBS and waiting for 2.5 hours with a mean=9834.3, SE(mean)=758.21.

Experiment 3 had a PBS baseline intensity mean=16984.29, SE(mean)=1589.18, a drop after removing PBS and adding Vectashield with a mean=2376.21, SE(mean)=247.32, and a recovery after replacing Vectashield with PBS and waiting for 2.5 hours with a mean=13369.76, SE(mean)=1367.025.

Separate ANOVA for AF488 in each of the 3 experiments

For dye AF488, there was also a main effect for imaging media in all 3 experiments, Experiment 1: $F(3, 76)=144.36$, $p<0.001$, partial $\eta^2=0.85$; Experiment 2: $F(3, 76)=160.66$, $p<0.001$, partial $\eta^2=0.86$; Experiment 3: $F(3, 76)=101.86$, $p<0.001$, partial $\eta^2=0.8$. Looking at the planned, post-hoc comparisons (Bonferroni), the same result was demonstrated in all three experiments: both Vectashield (PBS→VS) and 25 % Vectashield (PBS→25% VS) showed an increase in delta intensity, which was significantly different from the delta intensity of PBS and GLOX ($p<0.05$), while the delta intensities of PBS and GLOX did not differ significantly from each other. From our pilot work, we had assumed a medium effect size. We did not expect an effect as big as it turned out in our analysis, which came as a surprise to us. The effect was already big in experiment 1 and replicated in experiments 2 and 3. In detail, the results were as follows:

In experiment 1, there were no significant delta intensity differences between both PBS imaging media and between PBS and GLOX, but delta intensity showed an increase from PBS to Vectashield with a mean=3906.7 and an increase from PBS to 25 % Vectashield with a mean=9579.34, SE(means)=400.53 (with post-hoc Bonferroni $p<0.05$). The increase was stronger for 25% Vectashield than for Vectashield (with post-hoc Bonferroni $p<0.05$)

In experiment 2, there were no significant delta intensity differences between both PBS imaging media and between PBS and GLOX, and delta intensity showed an increase from PBS to Vectashield with a mean=1781.265 and an increase from PBS to 25 % Vectashield with a mean=10930.1, SE(means)=415.99 (with post-hoc Bonferroni $p<0.05$). The increase was once again stronger for 25 % Vectashield than for Vectashield (with post-hoc Bonferroni $p<0.05$).

In experiment 3, there were once again no significant delta intensity differences between both PBS imaging media and between PBS and GLOX, and delta intensity showed an increase from PBS to Vectashield with a mean=2297.175 and an increase from PBS to 25 % Vectashield with a mean=3959.1, SE(means)=199.99 (with post-hoc Bonferroni $p<0.05$). The increase was again stronger for 25 % Vectashield than for Vectashield (with post-hoc Bonferroni $p<0.05$).

Acknowledgements

This study is supported by the Emmy-Noether programme (project number 317530061 to INS) of the German Research Foundation and the Werner Reichardt Centre for Integrative Neuroscience (CIN) at the Eberhard Karls University of Tübingen. The CIN is an Excellence Cluster funded by the German Research Foundation within the framework of the Excellence Initiative (EXC 307).

Author Contributions

AA, NS and INS performed the experiments and analysis. AA and INS performed dSTORM imaging. RS performed the statistical analysis with the input from INS. INS designed the experiments with statistical advice from RS. INS wrote the manuscript with the input from AA, NS and RS. INS supervised the project.

Competing Interests Statement

The authors declare no competing interests.

References

1 Rust, M. J., Bates, M. & Zhuang, X. Sub-diffraction-limit imaging by stochastic optical reconstruction microscopy (STORM). *Nature methods* **3**, 793-795, doi:10.1038/nmeth929 (2006).

2 Huang, B., Bates, M. & Zhuang, X. Super-resolution fluorescence microscopy. *Annual review of biochemistry* **78**, 993-1016, doi:10.1146/annurev.biochem.77.061906.092014 (2009).

3 Heilemann, M., van de Linde, S., Mukherjee, A. & Sauer, M. Super-resolution imaging with small organic fluorophores. *Angewandte Chemie* **48**, 6903-6908, doi:10.1002/anie.200902073 (2009).

4 Dempsey, G. T., Vaughan, J. C., Chen, K. H., Bates, M. & Zhuang, X. Evaluation of fluorophores for optimal performance in localization-based super-resolution imaging. *Nature methods* **8**, 1027-1036, doi:10.1038/nmeth.1768 (2011).

5 Olivier, N., Keller, D., Rajan, V. S., Gonczy, P. & Manley, S. Simple buffers for 3D STORM microscopy. *Biomed Opt Express* **4**, 885-899, doi:10.1364/BOE.4.000885 (2013).

6 Cordes, T., Maiser, A., Steinhauer, C., Schermelleh, L. & Tinnefeld, P. Mechanisms and advancement of antifading agents for fluorescence microscopy and single-molecule spectroscopy. *Phys Chem Chem Phys* **13**, 6699-6709, doi:10.1039/c0cp01919d (2011).

7 Banterle, N., Bui, K. H., Lemke, E. A. & Beck, M. Fourier ring correlation as a resolution criterion for super-resolution microscopy. *Journal of structural biology*, doi:10.1016/j.jsb.2013.05.004 (2013).

8 Huang, B., Wang, W., Bates, M. & Zhuang, X. Three-dimensional super-resolution imaging by stochastic optical reconstruction microscopy. *Science* **319**, 810-813, doi:10.1126/science.1153529 (2008).

9 Schindelin, J. *et al.* Fiji: an open-source platform for biological-image analysis. *Nature methods* **9**, 676-682, doi:10.1038/nmeth.2019 (2012).

10 Linkert, M. *et al.* Metadata matters: access to image data in the real world. *The Journal of cell biology* **189**, 777-782, doi:10.1083/jcb.201004104 (2010).

11 Thevenaz, P., Ruttimann, U. E. & Unser, M. A pyramid approach to subpixel registration based on intensity. *IEEE Trans Image Process* **7**, 27-41, doi:10.1109/83.650848 (1998).